Analysis of residual plastic deformation of blanked sheets out of automotive aluminium alloys through hardness map

Analysis of residual plastic deformation of blanked sheets out of automotive aluminium alloys through hardness map

Analysis of residual plastic deformation of blanked sheets out of automotive aluminium alloys through hardness map

G Maculotti[1*], S Bonù[2], L Bonù[2], R Cagliero[3], G Genta[1], G Marchiandi[1] and M Galetto[1]

[1] Department of Management and Production Engineering, Politecnico di Torino, C.so Duca degli Abruzzi 24, Torino 10129, Italy
[2] AGLA Power Transmission, Via Avigliana 9, Avigliana 10051, Italy
[3] LBN Ricerca, Via Avigliana 2, Sant'Ambrogio di Torino 10057, Italy

*Corresponding author: giacomo.maculotti@polito.it

Abstract: Reducing overall vehicle weight is essential to reduce fuel consumption and pollutant emission and to improve noise, vibration, and harshness (NVH) performances. The substitution with lighter alloys can involve the grand majority of vehicle components, depending on the market sector. In several applications, e.g., chassis, pulleys, and viscodampers, metal sheets are formed in several steps, each of whom work-hardens the material reducing the available residual plasticity. Typically, the process is designed via FEM, whose results are affected by the initial conditions, often neglected, and is performed on pre-processed materials from suppliers. In this regard, correctly simulating the first step of the process is critical. However, the related initial conditions, in terms of residual stress and strain induced by former preliminary operations, are often neglected. This work proposes a quick and economical experimental procedure based on a hardness map to estimate initial conditions and to validate FEM results. The procedure allows evaluating the material's residual plasticity, which is necessary to process engineers to design following manufacturing steps. The approach is demonstrated on an industrially relevant case study, i.e., the blanking of an AA 5754, in use for water pump pulleys.

Keywords: Residual plastic deformation, Hardness map, Blanking, Aluminium, Automotive.

1. Introduction

The current regulatory framework is pushing the automotive sector to increased adoption of aluminium alloys to decrease the overall weight and enable fuel consumption and pollutant emission reduction [1,2]. Nowadays, substitution with lighter alloys for vehicles mainly targets chassis and body-in-white (BIW) for weight reduction (here including also multi-material solutions) [3,4]. In higher-end sectors, lightweighting targets transmission components, e.g., water pump pulleys and viscodampers, for benefits in power transmission regularity, durability, and efficiency in powertrain systems, reduction of inertial masses, and improved noise-vibration-harshness (NVH) and fuel consumptions performances [5,6]. As far as the latter is concerned, in the broadest sense, lightweighting can achieve the reduction of pollutant and greenhouse emissions [5] and allow improved design for electric vehicles and their batteries [7–9]. Substitution of steel with aluminium alloys in the automotive industry, e.g., for BIW, chassis, and transmission, allows targeting almost 70% of the overall vehicle weight [2].

Cold forming is a typical process for several components belonging to the above-mentioned assemblies. Automotive aluminium alloys for cold forming, usually from series 5000, can replace

conventional steels. A specific choice may consist in replacing conventional deep drawing steel DD13 with a lighter AA 5754. The latter is characterized by lower density, slightly smaller elongation, lower tensile strength, and generally more elastic behavior. This set of mechanical properties and the chemical composition reduce, with respect to steel alloys, the formability at environmental temperature, and challenges some joining operations, critical to guarantee stiffness and NVH performances, for example, in unibody chassis [2]. Also, aluminium alloys are more expensive, as raw material and from the processing perspective, but costs are well counterbalanced by the technical advantages and quality of the final product. Several of these applications require sheet metals to be formed in several steps (i.e., blanking, stamping, rolling). Each of these steps work-hardens the material and contributes to reducing the residual plasticity of the component. Blanking has been identified as a strategic process to reduce mechanical properties' scattering in finished products [10]. Reduced formability may promote cracks nucleation/propagation in critical zones of the product, thus shortening the fatigue life, which is core for power transmission components.

Quick and reliable experimental procedures to assess residual plastic deformation are scarcely available in the literature. Those available mainly rely on destructive uniaxial tensile tests and may not represent the actual processing condition and the local mechanical stress field inside the material. Moreover, given the material substitution and the processing complexity, the finite element method (FEM) is relied upon to simulate the manufacturing process to achieve optimization ultimately. However, validation of FEM results is necessary to guarantee the quality of results, reduce scraps, and limit process set-up time.

This work defines a novel methodology, based on hardness mapping, to estimate the residual plasticity of blanked aluminium alloys sheets and to validate the mechanical stress predicted by FEM results at once. The methodology is demonstrated on an industrially relevant case study, i.e., the blanking of AA 5754, in use for water pump pulleys. The rest of the paper is structured as follows. Section 2 describes the proposed methodology. Section 3 describes the industrial application and discusses the results. Section 4 finally draws conclusions.

2. Methodology

2.1. Damage criterion for residual plasticity

Cold forming of complex shapes, e.g., BIW components, chassis sections, water pump pulleys, requires performing several steps of forming and rolling on a semi-finished product. The former results from preliminary operations, e.g., rolling and blanking, on the raw material (usually processed in the form of coils). These introduce residual stresses in the component that affect subsequent cold forming operations. For a process consisting of several steps, the residual formability after each is a critical parameter for designing the following steps and assessing final component mechanical performances. In fact, each of those work-hardens the material reducing the available plasticity. Since the beginning of the past century, hardness has been used to estimate the yield strength, σ_y, by a non-destructive procedure alternative to the tensile test, additionally not requiring ad-hoc shaped specimens [11,12]. Amongst several hardness scales, Vickers hardness allows resolving and characterizing microstructures with sufficient lateral resolution. The relationship between Vickers hardness, *HV*, and σ_y depends on a material dependent parameter α, typically estimated by regression on experimental data [12,13]:

$$HV = \alpha \cdot \sigma_y \quad (1)$$

Falsafi and Demirci defined an approach to estimate the damage introduced by a processing step, i.e., the complement to the residual plasticity [14]. They exploited the variation of Vickers hardness in a processed material to identify the presence of residual stress, and conversely, the properties of unaffected material. This could be achieved by mapping the material in terms of Vickers hardness, which allows identifying the core region of material, i.e., where residual stress is negligible, characterized by the hardness H_0. Accordingly, they proposed an empirical damage criterion allowing to estimate the relative residual plasticity:

$$P_{Res} = 1 - \frac{HV}{H_0} \quad (2)$$

2.2. Empirical method for FEM validation

FEM simulations are exploited to design and subsequently optimize manufacturing processes. Setting up FEM is a non-trivial task that requires knowledge specific to the process and the simulation method. These are necessary to respectively choose the process parameters and the simulation options most adequately, e.g., dimension and type of the mesh. Moreover, FEM results are deeply dependent on the set-up and the material's parameters, constitutive equation, and the initial conditions, i.e., the state of the material at the beginning of the simulated process [15].

Validating FEM results is essential to reduce process set-up time and scraps and ultimately improve manufacturing efficiency and quality. However, influence factors must be strictly controlled to achieve this aim. Conversely, to maintain reasonable costs, methods to validate results and control influence factors shall be feasible, economical, and fast.

Simulation parameters depend on the accuracy degree targeted and the computational resources; they will not be discussed here.

Manufacturing conditions include geometry, e.g., the clearance allowance between the punch and matrix die, and boundary conditions, e.g., temperature, and processing parameters, e.g., for a blanking, the cutting force, die speed, force applied by the pressure pad, and the system's kinematic and dynamic. Here, we assume that manufacturing parameters are known, representing a trial run before optimization or carry-over. Therefore, influence factors related to the processed material ultimately control the results.

Elasto-plastic behavior of the material during a cold forming operation can be well described by Ludvick-Hollomon equation, see equation (3), or by Swift's model, see equation (4) in presence of a pre-strain [16]:

$$\sigma = K \cdot \varepsilon^n \quad (3)$$

$$\sigma = K \cdot (\varepsilon + \varepsilon_0)^n \quad (4)$$

where σ is the stress, ε the strain, ε_0 the pre-strain, K is the strength coefficient, and n the work-hardening coefficient. These parameters are typically not included in FEM software libraries, which often refer only to the material class. Consequently, tensile tests on the actual material to be process is advisable to either validate library values or to correct them, if necessary.

Modeling damage propagation is essential to describe accurately fracture numerically. Amongst several alternatives, the Rice-Tracey model. i.e.,

$$\dot{R} = R_0[\gamma\dot{\varepsilon} + D\dot{p}] \quad (5)$$

describes the nucleation, growth, and coalescence of micro-voids from an initial geometry R_0, depending on the shape variation γ, the strain gradient $\dot{\varepsilon}$, the volume variation D and the plastic equivalent deformation $\dot{p}$. The model is apt for cold forming as micro-voids have been proved to control plastic fracture, which is characteristic during blanking of ductile alloys (like AA 5754).

Identifying material's initial conditions, i.e., the possible presence of residual stresses from former processing operations, is critical. This notwithstanding, it is often neglected in literature [10,14,15,17]. This work proposes an empirical method to validate and improve FEM results based on hardness maps. The procedure has been developed to minimize the experimental effort and, inherently, assumes that the FEM-simulated process has also been performed physically. The approach exploits the results obtained by Falsafi and Demirci [14] and the well-known Tabor's relationship, i.e., equation (1). The former allows identifying the material's initial properties, i.e., H_0; the latter computes the related yield stress, which can be input in the FEM simulation as the initial condition.

FEM can be replicated, and results, including the effect of initial conditions, collected. These are exploited for actual validation. In most cases, FEM yields an equivalent plastic stress-strain status, (Y, φ^*). Because in the case of cold forming, (Y, φ^*) results from an anisotropic process different from the stress induced by a Vickers indentation, equations (3) and (1) cannot be applied directly. Tekkaya

[18] proposed a model, based on the formerly mentioned equations, to correlate the Vickers hardness to (Y, φ^*), resulting from a empirical observation of data collected on a variety of cold formed materials:

$$Y_{FEM} = K \cdot (\varphi^* - 0.112)^n \quad (6)$$

$$Y_{HV} = 9.81 \frac{HV}{2.475} \quad (7)$$

Comparing Y obtained by FEM, i.e., Y_{FEM}, with its empirical estimation based on Vickers hardness, i.e., Y_{HV}, through equation (7) enables the validation of the results.

3. Case study: AA 5754 for automotive application

The proposed methodology has been exploited to validate the FEM simulation of blanking operation on an AA 5457 disc. The operation is the first one to manufacture a component belonging to a water pulley assembly.

The FEM simulation has been performed on COLDFORM software. Manufacturing parameters were set up, considering: (i) geometrical constraints, e.g., the continuous contact of both the blanking punch and the blank holder with the billet; (ii) geometrical parameters, e.g., punch stroke (10 mm), clearance allowance (0.2 mm); (iii) dynamics of the punch and the blank holder, including friction modeled according to Coulomb law.

Ludvick-Hollomon constitutive equation parameters were validated by performing three standard tensile tests and comparing experimental results with the theoretical curve from COLDFORM's library. i.e. considering the values K = 407 MPa and n = 0.2488. The material's initial conditions were empirically inferred by performing a map of indentation on a blanked disc cross-section. A portion of the disc was preliminarily polished with abrasive papers and diamond paste (up to 1 μm); figure 1 shows the blanked component and the extracted specimen.

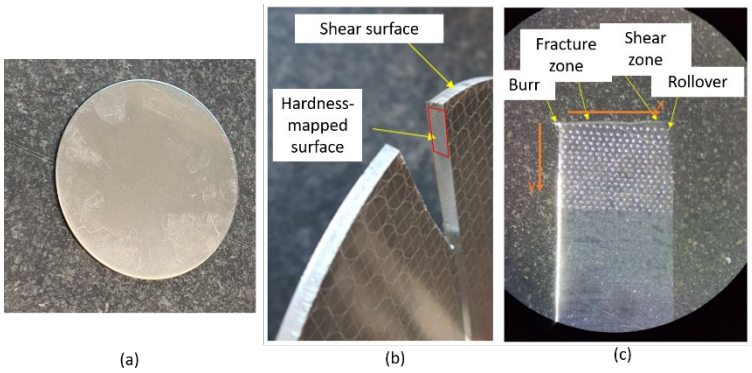

Figure 1. (a) Disc to be blanked; **(b)** Cross-section of the disc for extracting the **(c)** Sample on which hardness maps are performed.

Microstructural analysis was carried out by metallographic microscopy. Results show the presence of smaller and more stretched grains on the edge (figure 2(a)) than in the core (figure 2(b)) of the cross-sectioned specimen. The preliminary rolling underwent by the disc induces the difference. SEM and EDX were exploited to characterize the chemistry of the different phases. As far as different phases are concerned, globally, EDX showed, see figure 3, that in addition to the Al-Mg matrix, two intermetallic phases can be found, i.e., Mg2Si (black phase) and Al3(Fe, Mn) (white phase). Linear EDX was employed to study the presence of different alloying elements in the two main directions of the extracted specimen, i.e., longitudinally and transversally to the longer edges. No significant differences could be highlighted, concluding that differences in mechanical properties amongst the regions have to be sought in the grain dimensions and not in their chemistry, as per the Hall-Petch relationship [19].

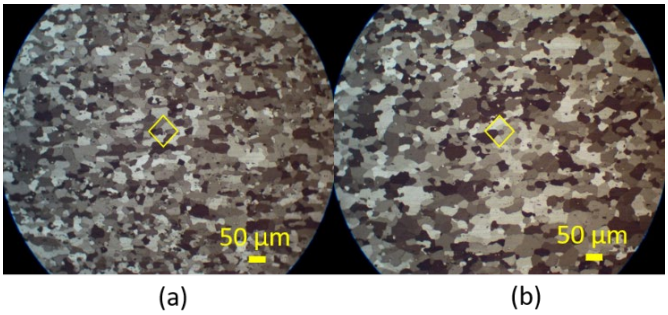

Figure 2. Metallography of **(a)** Edge, with smaller and more stretched grains, and **(b)** Core of the specimen. The diamond represents the size of a Vickers hardness indentation HV0.2.

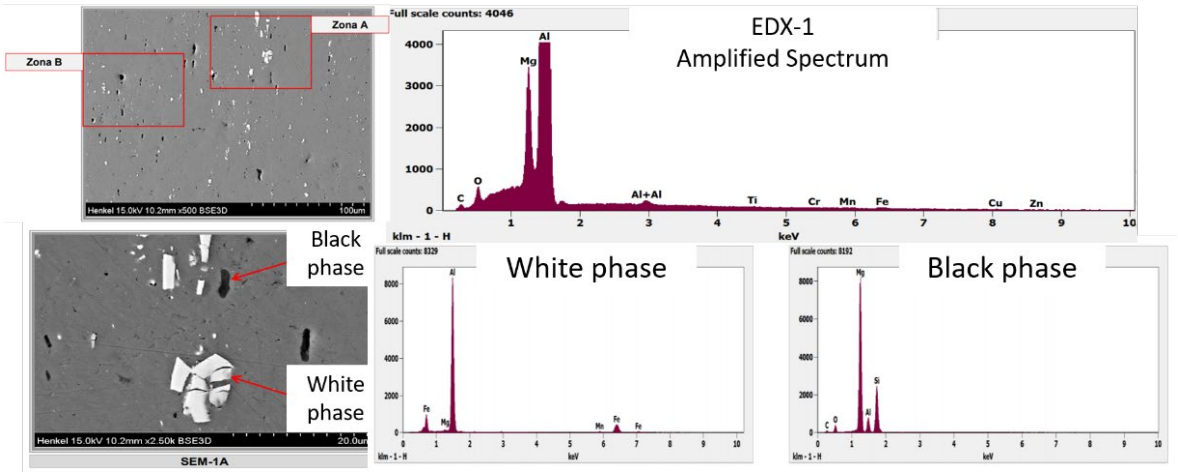

Figure 3. EDX to qualify the chemistry of the metallic matrix and intermetallic phases.

Vickers indentations at 0.2 kgf were performed [20] to cover a region of interest of (272×406) mm^2. Maps were replicated three times on three different cross-sections of the disc (at 0°, 45°, and 90° with respect to the rolling direction). Indentations' pace was at three times the diagonal, i.e., (3×78) µm, less than the standard requirement [20]. The non-standard choice aimed to provide high spatial resolution, representing average material properties. Analyses at the metallographic microscope guaranteed the latter showing that indentations covered more than five grains (see figure 3). Trial maps were performed at decreasing distance, i.e., 9-times, 6-times, and 3-times the diagonal, to validate the non-standard choice. No significant differences in hardness results were highlighted. This allowed concluding that the indentation-induced stress field was not impacting the results.

Figure 4(a) shows the HV trend in the indented region. The hardness is maximum in the neighborhood of the burr. It decreases, along the y-axis, to a minimum value independent from the distance from the shear surface is detected, i.e., H_0. Conversely, it is dependent on the distance from the plane surface of the disc, i.e., along the x-axis, due to former roll milling. Thus, the inner five hardness profiles were averaged to obtain the reference H_0 profile. This was used, by employing equations (1) and (3), to obtain pre-strain values that define the initial conditions, shown in figure 4(b), which can be input in the FEM software.

Subsequently, the FEM simulation is run, with geometry represented in figure 4(c). A volume mesh was set up to comply with the empirical resolution, for the sake of simplicity, at three times the average indentation diameter, i.e., triangular elements with size 0.2 mm at the shear surface. Obtained results in terms of equivalent strain are shown in figure 4(d).

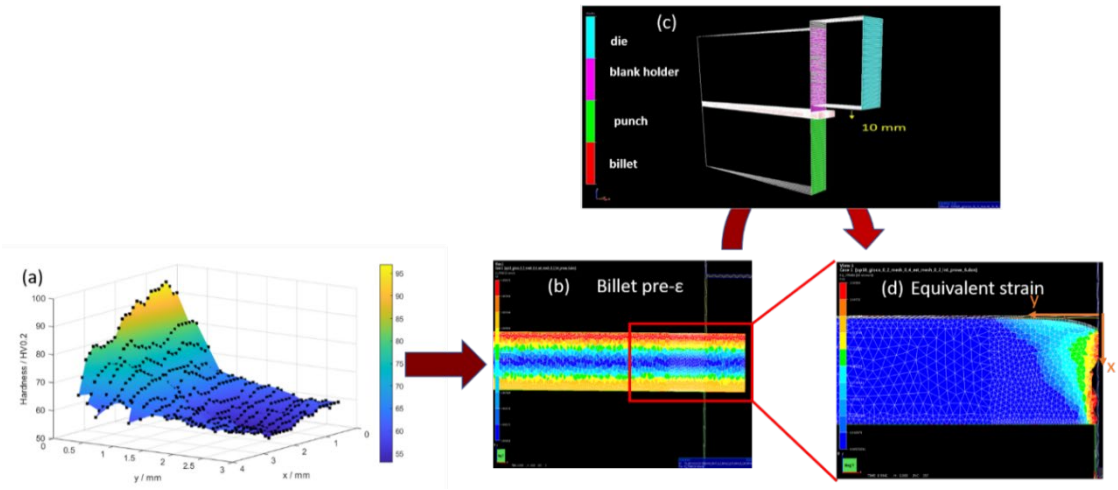

Figure 4. (a) Vickers hardness map enabling the identification of H0. (b) Resulting initial condition of strain, (c) Geometry of the simulated system (axial symmetry is exploited) and (d) Resulting FEM strain result.

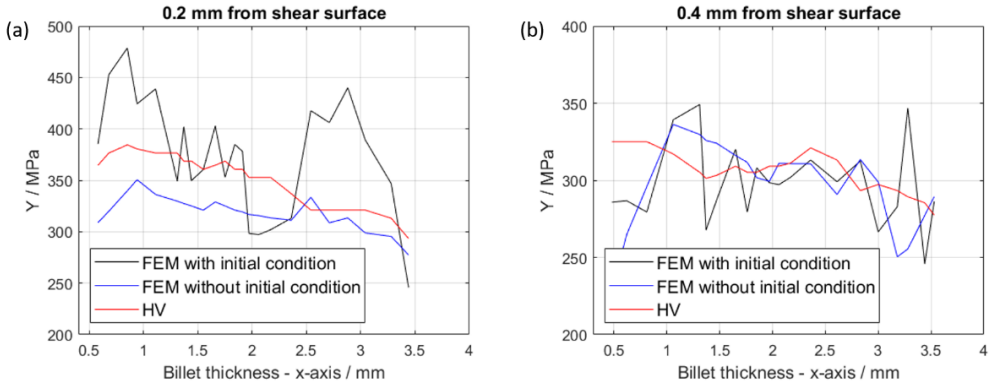

Figure 5. Comparison of flow stress obtained by FEM and by empirical measurement based on Vickers hardness to validate FEM results obtained with and without initial condition at **(a)** 0.2 mm and **(b)** 0.4 mm from the shear surface.

The validation is carried out according to the discussion of Section 2.2 by comparing Y_{FEM} and Y_{HV}. The former, i.e., the equivalent stress obtained by the FEM, is obtained by applying equation (5.1) on the FEM strain results; the latter is the stress empirically estimated through the hardness by equation (5.2). Results are shown in figure 5, considering two representative distances from the shear surface, i.e., 0.2 mm and 0.4 mm. When initial conditions are included, differences can be ascribed to random factors, e.g., measurement noise. In fact, normal probability plot, shown in figure 6, and Anderson-Darling test on that differences cannot highlight systematic differences at a 95% confidence level.

When initial conditions are not included in the FEM simulation, results are significantly offset from empirical estimates, see figure 5 and figure 6. Figure 6 shows this systematic difference is attenuated toward the core of the material and confirmed quantitatively by ANoVA. Finally, according to equation (2), the residual plasticity is computed; results are shown in figure 7, highlighting that, on the shear surface's edge, a significant decrement of available plasticity is introduced by blanking, consistent with the significant simulation results improvement obtained introducing the pre-strain.

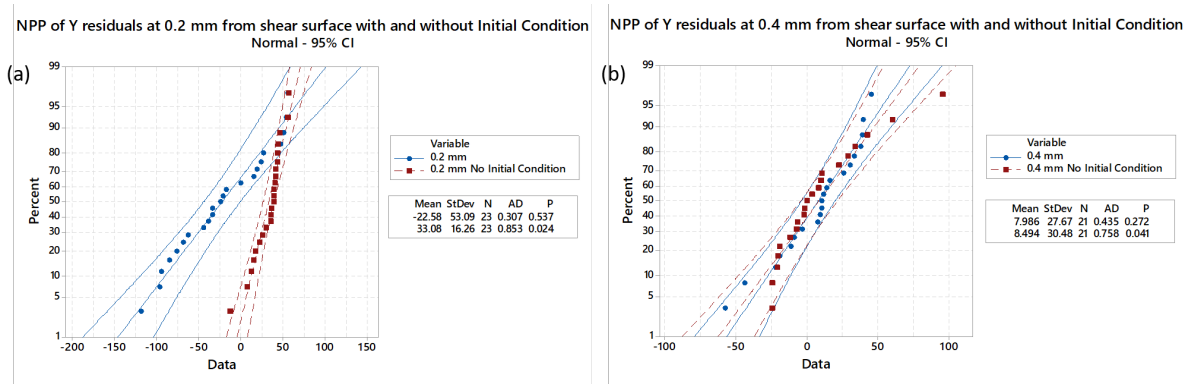

Figure 6. NNP of the difference between Y_{FEM} and Y_{HV} depending on the initial conditions in FEM simulation at **(a)** 0.2 mm and **(b)** 0.4 mm from shear surfaces. When initial conditions are disregarded, significant differences are highlighted, that cannot be ascribed to random factors with a risk of error of 5%. Differences are less relevant at greater distance from the shear surface.

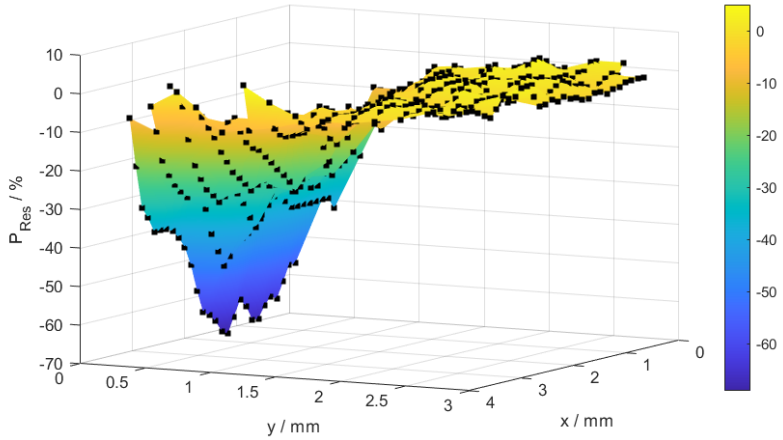

Figure 7. Relative residual plasticity: significant decrement of available plasticity is introduced by blanking on the edge of the shear surface.

4. Conclusions

This paper presented an empirical and reliable methodology to validate FEM simulation of metal forming. The proposed procedure, which is valid for any metallic material and metal forming process, was successfully tested for aluminium blanking. This operation is critical for the cold forming of this material in several automotive applications. The paper showed that, by hardness map, FEM simulation can be improved by defining initial conditions. Moreover, by the same means, FEM can be validated and a reliable estimate of residual plasticity of the material obtained. This parameter is essential to allow the effective design of subsequent manufacturing process steps. The FEM validation achieved by the method herein proposed allows optimizing the process by modifying process parameters and limiting subsequent additional experimental testing, with cost and time reduction. Moreover, it would allow monitoring changes of surface mechanical properties due to further complex manufacturing processes, which is essential, for example, when product engineers need to test fatigue life. Last, it is noteworthy that the procedure here devised allows reverse engineering elementary manufacturing processes, e.g., blanking, by FEM simulation, bounding the results to experimental case studies.

Acknowledgments

This work results from a collaboration between the laboratories of LBN Ricerca and Politecnico di

Torino's Quality Engineering and Management Group. The authors would like to thank Miss Maria Chiara Casavecchia and Mr. Carmine Palladino for the support and the effort endeavored in collecting and analyzing data.

References

[1] Tucker R 2013 Trends in automotive lightweighting *Metal Finishing* **111** p 23–25
[2] Tisza M and Czinege I 2018 Comparative study of the application of steels and aluminium in lightweight production of automotive parts *International Journal of Lightweight Materials and Manufacture* **1** (4) pp 229-238
[3] Henriksson F and Johansen K 2016 An Outlook on Multi Material Body Solutions in the Automotive Industry - Possibilities and Manufacturing Challenges *SAE Technical Papers* 2016-01-1332
[4] Cecchel S, Ferrario D, Panvini A and Cornacchia G 2018 Lightweight of a cross beam for commercial vehicles: Development, testing and validation *Materials and Desing* **149** pp 122-134
[5] Kulkarni S, Edwards D J, Parn E A, Chapman C, Aigbavboa C O and Cornish R 2018 Evaluation of vehicle lightweighting to reduce greenhouse gas emissions with focus on magnesium substitution *Journal of Engineering Desing and Technology* **16** pp 869-888
[6] Wilhelm E, Hofer J, Schenler W and Guzzella L 2012 Optimal implementation of lightweighting and powertrain efficiency technology in passengers' vehicles *Transport* **27** pp 237-249
[7] Li Z, Duan L B, Cheng A G, Yao Z P, Chen T and Yao W 2019 Lightweight and crashworthiness design of an electric vehicle using a six-sigma robust design optimization method *Engineering Optimization* **51** pp 1393-1411
[8] Burd J T J, Moore E A, Ezzat H, Kirchain R and Roth R 2020 Improvements in electric vehicle battery technology influence vehicle lightweighting and material substitution decisions *Applied Energy* **283** p 116269
[9] Millo F, Cubito C, Rolando L, Pautasso E and Servetto E 2017 Design and development of an hybrid light commercial vehicle *Energy* **136** pp 90-99
[10] Ghiotti A, Bruschi S and Regazzo P 2014 Shear surface control in blanking by Adaptronic Systems *Procedia Engineering* **81** pp 2512-2517
[11] Small L 1960 *Hardenss, theory and practice* (Novi, MI: Service Diamond Tool Co).
[12] Tabor D 1951 *The hardness of metals* (London, UK: Oxford University Press).
[13] Maculotti G, Genta G, Lorusso M and Galetto M 2019 Assessment of heat treatment effect on AlSi10Mg by selective laser melting through indentation testing *Key Engineering Materials* **813** pp 171-177
[14] Falsafi J and Demirci E 2016 Micro-indentation based study on steel sheet degradation through forming and flattening: Toward a predictive model to assess cold recyclability *Materials and Design* **109** pp 456-465
[15] Klocke F, Beck T, Hoppe S, Krieg T, Müller N, Nöthe T, Raedt H-W and Sweeney K 2002 Examples of FEM application in manufacturing technology *Journal of Material Processing Technology* **120** (1-3) pp 450-457
[16] Swift H 1952 Plastic instability under plane stress *Journal of Mechanics and Physics of Solids* **1** pp 1-18
[17] Romano D, Vicario G and Galetto M 2000 Robust FEM Experiments *Proc. 3rd Int. Conf. Quality Reliability and Maintenance* p 171
[18] Tekkaya A E 2000 An improved relationship between Vickers hardness and Yield Stress for cold formed materials and its experimental verification *CIRP Annals* **49** pp 205-208
[19] Hansen N 2004 Hall-Petch relation and boundary strengthening *Scripta Materialia* **51** pp 801-806
[20] ISO 6507-1: 2018 *Metallic materials - Vickers hardness test* (Genève: ISO)